Computer Science
Technical Report

Colorado State University

Introduction to Computational Neural Modeling for Computer Scientists and Mathematicians

Keith A. Bush and Charles W. Anderson

January 12, 2004

Technical Report CS-04-101

Computer Science Department
Colorado State University
Fort Collins, CO 80523-1873

Phone: (970) 491-5792 Fax: (970) 491-2466
WWW: http://www.cs.colostate.edu

Introduction to Computational Neural Modeling for Computer Scientists and Mathematicians

Keith A. Bush and Charles W. Anderson

January 12, 2004

Contents

Abstract

The rise in availability of powerful personal computers allows researchers in many different disciplines access to problems that were, in the recent past, computationally intractable. Biologically realistic neural models are one example of a problem that is both computationally expensive, but also multidisciplinary by nature. These neural models incorporate fundamental neuroscience principles into a mathematical framework that may be understood and studied by experts in computer science and mathematics. Moreover, the inclusion of these disciplines into neural modeling research is essential as the models grow larger, more detailed, and hence more complicated in both construction and analysis. Neural modeling demands collaboration among widely differing scientific disciplines and thus, demands an easily accessible introduction to researchers grounded in the mathematical sciences. This introduction attempts to simply and succinctly introduce the basic biological, chemical, and physical science upon which neural models are built. The introduction then defines, derives, and explains, stepwise, numerical integration of the compartment model using the Backward Euler method.

1 Introduction

Computational neuroscience is the study of neurological function via mathematical models. A precise definition is more ambiguous. The methodology used in constructing mathematical neural models vary as widely as the questions to be answered. Some models implement potentiation to understand biological learning mechanisms. Other models may intend to reproduce anatomical data acquired from living tissue or reproduce electrophysiological recordings measured *in vitro*. Models may be inaccurate or highly accurate, small or large, from a single neuron to an entire sub-organ. The methods of spatio-temporal approximation, numerical analysis, and synaptic connectivity all may differ. However, the diversity of these models does not displace their commonality. All computational neural models are mathematical approximations of some unknown perfectly accurate and precise model of the brain. Therefore, computational neuroscience very much depends upon knowledge of both neuroscience and mathematics. The field of computer science performs the role of intermediary. Computer science techniques and technology enable the application of mathematical ideas as well as representation and analysis of model behavior and function. The following principles govern what should be considered well-practiced neural modeling.

- Knowledge of neuroscience principles
- Knowledge of computational time and space complexities
- Knowledge of numerical integration techniques
- Well-formed, realistic hypotheses
- Well-researched neurological parameters
- Awareness of computational resources
- Well-planned and implemented model design
- Documentation discipline (both parameter sources and coding)
- Knowledge of statistical analysis techniques
- Patience

You should note that principles of the study of neural modeling are rooted in principles of good science. Without these basic elements, neural modeling efforts will falter. Modeling the brain without direction will be fruitless. The topic is too vast. The interactions are too complex. The biological parameters required are often unknown or riddled with uncertainty. Alas, neural modeling is a desperate and often discouraging endeavor, yet the reward of discovery, and the priceless knowledge gained make it a worthwhile pursuit.

This paper briefly discusses the basic principles of neural modeling as a means to introduce advanced undergraduate and graduate computer science and mathematics students to the field. Fundamental biology, physiology, and chemistry components are presented as simply as possible. These introductions weave a thread of scientific foundation on which computational modeling may be built. Non-computational details are intentionally oversimplified to prevent distortion of the overall modeling message. The reader is encouraged to self-study the citations for greater depth of knowledge.

The paper is organized as follows. Section 2 introduces basic neuroscience principles. Physical and mathematical principles governing a single, linearly approximated neural model without synaptic connections or branches are presented in Section 3. The reader should pay specific attention to derivations provided for numerical integration of the compartment model as given in Section 3.6.

2 Neuroscience Principles

The neuron is the backbone of information processing in the brain. However, by itself a single neuron has limited processing capability. The brain contains uncountable variations of neural networks, systems of interconnected neurons, to satisfy a wide range of processing needs. To understand how neural networks

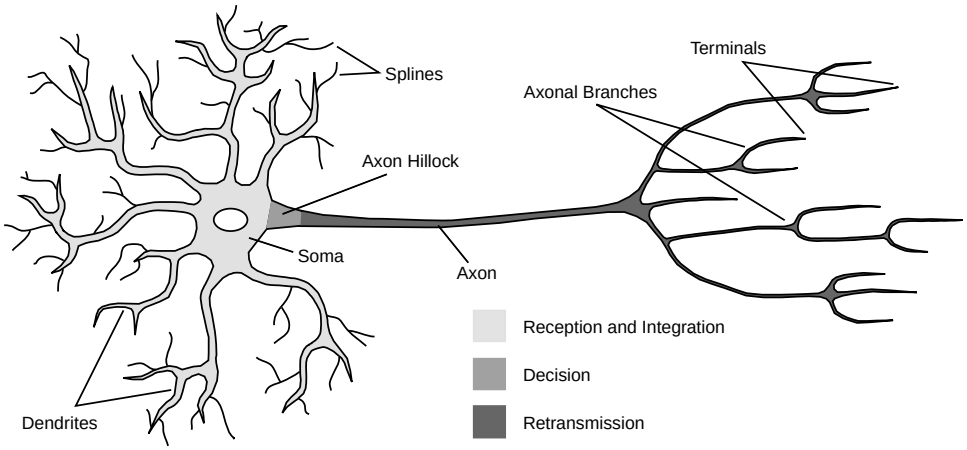

Figure 1: Generalized depiction of a neuron.

serve as information processors, however, one must understand the anatomical and physiological architecture of a simple neuron first. Only then can the role of complex interconnectivity be understood as a cohesive functional unit.

2.1 The Neuron

From an information processing perspective, the purpose of the neuron is to receive, process, and retransmit signals. Signals, in this context, are disruptions in the membrane potential of the neuron. A neuron, for reasons to be discussed later, maintains an electrical potential across its membrane of approximately -60 to -70 mV. Because the equilibrium potential is negative, the neuron is said to be hyperpolarized with reference to the extracellular space. Signals generally take the form of depolarization, positive change, of the membrane potential. Depolarizing changes propagate across the neural membrane such that a depolarization at a dendritic branch will propagate to the axon hillock. Membrane depolarizations have a second property, they are additive. For example, a depolarization of 15 mV occurring adjacent to a depolarization of 20 mV causes the locations between to have a depolarization of some linear combination of these values, greater than either value individually ($\geq$ 20). Neural anatomy is configured to take advantage of membrane potential changes to convey and process information. A generalized neuron is depicted in Figure 1 to aide in the discussion of anatomical functionality.

At a high-level, neural anatomy may be decomposed into five sections: the dendritic tree, the soma, the axon hillock, the axon proper, and axonal branches. Functionally, however, the neuron has three sections: reception and integration, decision, and retransmission. Information is received in the dendritic tree via synaptic connections. Details of the synapse will be provided later, but initially, we can think of synaptic connections as physical locations where inbound signals are collected by the neuron. All signals propagate to the axon hillock where their effects are summed. If the summed depolarizations, via the additive property, achieve a fixed threshold depolarization, an action potential occurs. An action potential is defined as an all-or-none, massive depolarization of the neural membrane. The axon and axonal branches serve the purpose of transmitting the action potential over long distances and to many different locations. To aide understanding, a graphic depicting a generalized neuron in provided in Figure 1.

With this high-level description in place, the underlying information processing functionality of the neuron is available for study. The highly complex branching structure of the dendritic tree serves to collect numerous incoming signals from many different neurons. Due to passive propagation and additive properties of the membrane depolarizations occurring at synaptic connections, the dendritic tree can be viewed as a giant antennae that collects signals. As signals propagate down the branch structure they are summed at intersections. The entire dendritic tree, may be referred to as the signal collection component.

As signals propagate down the dendritic tree, they eventually reach a single terminus, the axon hillock.

All signals are summed at this location. Therefore, the axon hillock may be viewed as the signal integration component. However, the axon hillock does not just passively sum incident signals. This section of the neural membrane contains a high density of voltage-gated ion channels. These channels have the effect of magnifying membrane depolarizations should the passive sum of the depolarization achieve some value above a fixed threshold value, which varies from neuron to neuron. In a very basic way, the combined effects of the voltage-gated ion channels in the axon hillock form a binary switch. When summed membrane depolarization is below some value, the switch remains off, and passive propagation continues through the axon hillock and down the axon. However, if the summed depolarization reaching the axon hillock achieves a value greater than (i.e. less negative than) the threshold, the the switch is turned on. Turning on the switch is equivalent to generating an action potential, a massive depolarization, of approximately 100 mV.

The axon and axonal branches have the duty of transmitting action potentials to various locations in a neural network. The axon, via its natural myelin sheath insulation, is capable of transmitting action potentials over large distances, quickly, and with little loss of potential. Some axons can be as long a one meter and achieve signal transmission velocities of 1 m/s. Axonal branches may carry the action potential to several thousand other neurons.

2.2 The Synapse

The synapse is the location of transfer between neurons. Formally, the synapse is empty space separating the axonal terminal of the presynaptic neuron with the dendrite of the postsynaptic terminal. Unlike signal propagation within a neuron, signal transmission between neurons occurs via chemical signaling. At a high-level, the process is comprised of discrete, sequential steps. First, an action potential must propagate to the axonal terminal of the presynaptic neuron. The depolarization of the membrane caused by the action potential causes vesicles containing neurotransmitters to bind to the membrane of the presynpatic axonal terminal. These vesicles then rupture, releasing neurotransmitter into the empty space separating the presynaptic and postsynaptic neurons, properly called the synaptic cleft. Neurotransmitters diffuse across the synaptic cleft and bind to neurotransmitter specific receptors located on the dendritic membrane of the postsynaptic neuron. These receptors in turn cause ion-channels to open, allowing diffusion of ions across the postsynaptic neural membrane, depolarizing the membrane. Propagation of the signal then proceeds passively as described previously. Neurotransmitter is absorbed by surrounding support cells, specifically astrocytes. Vesicles are filled and repaired in the neuron nucleus. Slow transport processes are responsible for moving vesicles containing neurotransmitter from the nucleus to the axonal branches as well as returning ruptured vesicles for repair and refilling.

The type of neurotransmitter released by the presynaptic neuron governs the function of the synaptic connection. Synaptic connections are classified in two ways, excitatory and inhibitory. Excitatory synapses cause depolarization of the postsynaptic neuron. Inhibitory synapses hyperpolarize the postsynpatic neuron, or secondarily, block the function of nearby excitatory synapses. The type of neurotransmitter and the functionality of the postsynaptic receptor govern this classification. While hundreds of neurotransmitters have been discovered, the four most significant types are defined below:

- **AMPA** (*alpha-amino-3-hydroxyl-5-methyl-isoxazole-4-proprionate*), fast excitatory
- **NMDA** (*N-methyl-D-aspartate*), slow excitatory
- $\mathbf{GABA_A}$ (*gamma-aminobutyric acid, A-type*), fast inhibitory
- $\mathbf{GABA_B}$ (*gamma-aminobutyric acid, B-type*), slow inhibitory

The fast and slow specifications above concern the rate at which depolarization or hyperpolarization is induced in the postsynaptic neuron. Fast synapses may cause potential change in $1-3$ ms. Slow synapses may effect potential changes over $20-40$ ms. Speed of influence and excitatory or inhibitory behavior differ widely among known neurotransmitters. For greater detail readers are directed to Kandel, Scwhartz, and Jessell Kandel et al. (1991).

2.3 Neural Networks

The process of signal collection, integration, and retransmission within a single neuron has been shown to be equivalent to a non-linear function. A collection of neurons, given certain assumptions, can then be shown to be mathematically equivalent to a linear combination of non-linear functions. Theoretically, any function may be approximated via a linear combination of non-linear functions, given enough non-linear functional elements exist.

While the exact role of the entire brain has not been determined, the functionality of subsections has been determined experimentally. Details of these analysis are beyond the scope of this paper.

3 Neural Modeling Principles

3.1 Membrane Potential

Neurons convey information via electrical and chemical signals. Neural membrane potential is the mechanism by which this signal information is conveyed. As discussed previously, an overly simplified neuron is a lipid-bilayer compartment of intra-cellular fluid, cytoplasm, bathed in extracellular fluid. Both intra-cellular and extracellular fluid types contain concentrations of various ions, particles carrying net positive charge (cations) and net negative charge (anions). For the purpose of explanation, we will propose that these fluid contain significant concentrations of only two ionic species, potassium and sodium. The extracellular fluid contains a relatively greater concentration of sodium ions, Na^+, and the cytoplasm contains a relatively greater concentration of potassium, K^+, ions. Both fluid types contain mixtures of these two ionic species.

This system, a barrier separating solutions of differing concentrations of ionic species, is the definition of a battery. We know intuitively that batteries are sources of electrical potential and current. Given this perspective, we may define membrane properties by means of electromagnetic. Ohms Law is the relationship governing these basic relationships and is defined by the following equation.

$$V = I \cdot R \tag{1}$$

where V denotes potential (Volts), I denotes current (Amps), and R denotes resistance (Ohms). Potential is directly proportional to current and resistance. Thus, potential may be thought of as the driving force of current. Current is the movement of charged particles through a circuit. Resistance represents the opposition of current in a circuit.

It is well known that all neural membranes possess a multitude of ion-selective channels that facilitate the diffusion of ions across the membrane barrier. Unique channel types vary by the thousands if not millions. However, for simplicity we consider only passive, non-gated channels selective to one of the two species available, Na^+ or K^+. These channels allow electro-chemical forces to drive ionic transfer across the barrier via diffusion. The existence of ionic flow across the membrane defines what is called ionic current, I_{ion}. As with electrical circuits, ionic current and membrane potential behave according to Ohms Law.

With Ohms Law behind us, we can now investigate well-understood theory to explain the relationship between ionic concentrations, membrane potential, and ionic current. However, we must abstract further for clarity. Consider temporarily that the neural membrane is impermeable to Na^+. This is equivalent to stating that the membrane's resistance to Na^+ ion diffusion is infinitely large, which by Ohms law would make Na^+ potential equal to zero. Therefore, only K^+ ions may transfer across the membrane and the electro-chemical potential across the membrane, at equilibrium, may be described by the Nernst Equation:

$$E_K = \frac{RT}{ZF} \ln \frac{[K^+]_o}{[K^+]_i} \tag{2}$$

where R is the ideal gas constant, T is temperature, F is the Faraday constant, and Z is the effective valence of K^+. Thus, if we consider equilibrium conditions to have constant temperature then $\frac{RT}{ZF}$ is constant and equilibrium depends only on the natural logarithm of the quotient of K^+ ionic concentration outside and inside the membrane, respectively. Further, when extracellular and intra-cellular K^+ concentrations are equal, it is obvious that $E_K = 0\ mV$.

Detailed experimental measurements have determined $E_K = -75\ mV$. This result demands one further explanation. Neurons normally carry net negative charge within the cell and net positive charge externally.

Canonically, notation describing membrane potential as positive or negative assumes that negative potential indicates excess intra-cellular negative charge, although it should be obvious that the opposite convention would also be appropriate.

For completeness, the Nernst Equation describing potential generated by separation of extracellular and intra-cellular Na^+ ions given that the membrane is impermeable to K^+ ions, follows:

$$E_{Na} = \frac{RT}{ZF} \ln \frac{[Na^+]_o}{[Na^+]_i} \tag{3}$$

E_{Na} has been determined experimentally to be approximately $+55\ mV$. Again, note the relative nature of this number, indicating that a significant net positive charge exists extracellularly. The realistic neural membrane is more complex. A normal neuron contains passive channels permeable to both K^+ and Na^+ ions. Fortunately, equilibrium potential for the influence of multi-species, non-gated channels is well-understood and described by the Goldman Equation as follows:

$$V_m = \frac{RT}{F} \ln \frac{p_K[K^+]_o + p_{Na}[Na^+]_o}{p_K[K^+]_i + p_{Na}[Na^+]_i} \tag{4}$$

where p_K and p_{Na} are membrane permeabilities to K^+ and Na^+ ions, respectively. These values may be thought of as the relative densities of open-gated, ion specific channels present in the membrane for each ionic species. Thus, the Goldman Equation can be thought of as a more generalized version of the Nernst Equation. In fact, if the permeability of one species is set to zero, then the Goldman Equation reduces to the Nernst equation for the remaining species.

A question should arise in your mind at this point. Both the Nernst Equation and Goldman Equation describe the equilibrium potential achieved when concentrations of ionic species are maintained on opposite sides of the membrane. However, we also state that non-gated channels exist that allow diffusion of ionic species across the barrier. If this is the case, then any equilibrium condition cannot be maintained as ions flow from high concentration to low concentration. This diffusion of ions down the concentration gradient will drive the membrane potential to $0\ mV$. How is this possible?

Thankfully, the answer is well understood. All neurons contain a metabolic process called the $Na^+ - K^+$ pump. The $Na^+ - K^+$ pump functions to maintain net negative charge in the intra-cellular space. This is achieved by a chemical process in which 3 Na^+ ions are transported out of the neuron and 2 K^+ ions are transported into the neuron with the hydrolysis of ATP Kandel et al. (1991) as the result. Thus, equilibrium concentrations in the extracellular and intra-cellular space are maintained. The imbalance of Na^+ to K^+ transfer during the $Na^+ - K^+$ pump cycle has an additional effect. The unequal 3-2 transfer of cations across the membrane forces additional K^+ ions to diffuse across the membrane into the neuron, forming an net ionic current at equilibrium. The current is often called *leak*.

Experimental measurements have shown that neural membranes in which only non-gated Na^+ and K^+ channels account for ionic diffusion have an equilibrium membrane potential,V_m, of approximately -60 to $-70\ mV$. Canonically, the membrane potential in this configuration is defined as the resting potential denoted, E_{rest}. Given this very negative membrane potential it should be clear from the Goldman Equation that the permeability of K^+ channels dominates that of Na^+ channels when at resting equilibrium.

Another important topic of discussion, one that will be raised many times later in this paper, is the understanding of how the rest potentials relate to ionic current. The E_{Na}, E_K, and E_{rest} potentials may be thought of as theoretical batteries driving ionic currents in and out of the neuron as stated by Ohms Law. At steady-state, E_{rest} acts as the combined driving force of ionic current, which as was discussed, is dominated by relatively high passive K^+ diffusion across the membrane (high K^+ ion permeability). E_{rest} is slightly depolarized from E_K due to the effects of membrane permeability of Na^+ ions as described by the Goldman Equation.

3.2 Passive Membrane Properties

The brain's purpose is to generate, disseminate, and process signals. We define a signal to be a unit of information. In the case of biological neurons, the physical manifestations of the signal are magnitude and rate of change of membrane potential. In the previous section we learned how membrane potential is defined

at steady-state, physiologically based, and how Ohms Law determines the relationships between potential, current, and resistance. This section developed understanding of how the magnitude of membrane potential is determined. The rate of change of potential, with respect to time or space, requires further investigation.

Before we move onto these topics, however, we must discuss another electromagnetic concept that is critically important in neural function, capacitance. Capacitance is the ability to store and release charge. Capacitance relates to potential by the following equations:

$$V = Q/C$$

$$\Delta\ V = \Delta\ Q/C$$

where C is capacitance, V is potential, Δ V is change in potential, Q is charge, and Δ Q is the change in charge stored on the capacitor. To understand the role of capacitance in membrane potential rate of change, let us assume that the membrane is a capacitor in addition to being a resistor as described in the previous section. Given this, the charge carried by membrane current, I_m, must be decomposed into two pieces, ionic current, I_i, and capacitive current, I_c, related by the following equation:

$$I_m = I_i + I_c$$

The ionic current, as described previously, is defined by the net ionic diffusion across the membrane and behaves as described by Ohms Law. Capacitive current, however, has the property of adding and removing charge stored on the membrane itself. An outward capacitive current would then be described by the addition of cations to the intra-cellular surface of the membrane and removal of an equal number of cations from the extracellular surface. This is analogous to storage of current that flows in the opposite direction. The remainder of the section describes how the membrane's capacitive properties influence potential rates of change through both time and space.

3.2.1 Membrane Potential Temporal Rate of Change

The equation governing the rate of change of membrane potential with respect to time is given below:

$$\Delta V_m(t) = I_m R(1 - e^{-t/\tau})$$

where t denotes time and τ denotes the membrane time constant, a dimensionless quantity defined as the time required for the membrane potential to reach 63% of the value induced by a disruption of membrane current. An obvious observation follows. Given a command current, a step of current applied externally to the membrane, the membrane potential response behaves as a bounded non-linear function of time governed by the membrane time constant. Related time signatures exist within the ionic and capacitive components of the membrane current as shown in Figure 2.

The lower plot of Figure 2 depicts a step of command current as well as the ionic, I_i, and capacitive, I_c, components with respect to time. The superposition of I_i and I_c comprises the total current, I_m. This behavior is intuitive by the equation of membrane current provided above. More subtle, and important, is the behavior of membrane potential with respect to time as is given in the upper plot of Figure 2. Membrane potential change with respect to time (plot c) is non-linear as is shown by plot c. Figure 2 is important, however, in that it shows how the non-linear nature of potential change arrives from the interplay of resistive and capacitive properties of the membrane. Given the command current of the lower plot, line a depicts potential change behavior if the membrane contained only resistive properties. In this case the potential change would be instantaneous and maintain a constant value throughout application of the command current. Line b depicts change if the membrane were purely capacitive. Capacitive potential response is linear, and potential increases as the capacitor is charge. Once command current is released, the upper plot of Figure 2 depicts how potential non-linearly returns to the initial level. The lower plot reveals how stored capacitor charge is released in the absence of command current. A negative current, symmetrical to the capacitive current during application of command current, is released. This current is exactly opposed by the ionic current, creating a net zero membrane current. The two plots of Figure 2 fully specify the temporal nature of potential rate of change, showing how both resistive and capacitive properties of a neural membrane influence this change.

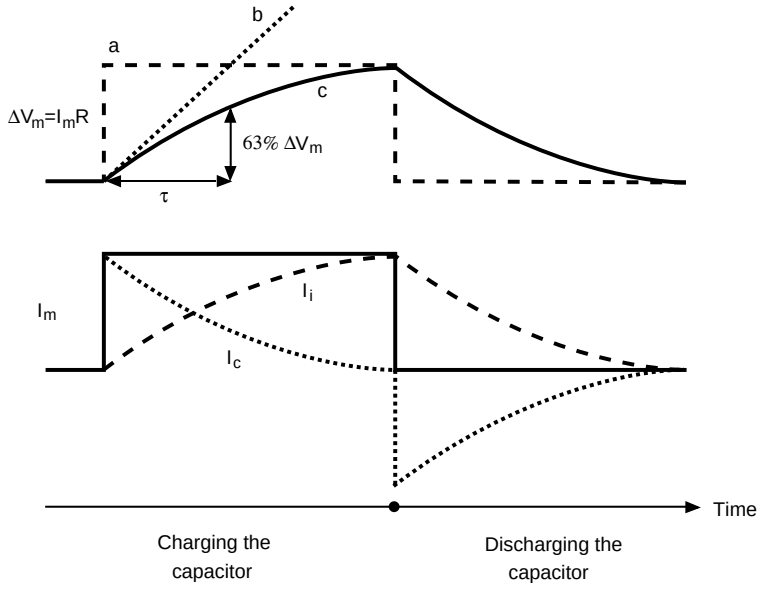

Figure 2: Membrane potential temporal response to current perturbation.

3.2.2 Membrane Potential Change through Space

A passive neuron behaves much like a wire cable used to transfer electricity. Ohms Law states that potential induces current. In our discussion, potential across the neural membrane induces ionic and capacitive current across the membrane, where membrane resistance, R_m, dissipates ionic current. When viewed as a cable, however, axial transfer of potential also occurs. That is, the potential at any point along the cable effects the potential at locations differentially proximal and distal to some fixed reference point. The relationship between potential, current, and resistance therefore applies spatially. Axial resistance, R_a, describes the dissipation of current induced by a potential as it propagates down the cable. As a property of conservation, current flows in the direction of least resistance. Therefore, a current applied to a point along the cable has two potential avenues of flow, ionic current across the membrane or propagation down the cable length. The following equation describes potential as a function of distance.

$$\Delta V_m(x) = \Delta V_o e^{-x/\lambda}$$

where V_o denotes the potential change at some point, x_o, x is the distance from the location of command voltage, and λ is the length constant, defined by the following relationship:

$$\lambda = \sqrt{\frac{R_m}{R_a}}$$

where λ is equivalent to the distance from the point of current application where ΔV has decreased by 63%. A spatial description of potential change with respect to distance can be seen in Figure 3.

Given these relationships governing the spatio-temporal rates of change of membrane potential, we have a clear view of passive neural membrane behavior. Passive neural behavior is most commonly seen in the dendritic branches of the neuron where voltage-gated ion channels are sparse or nonexistent.

3.3 Active Membrane Properties

We have limited our discussion to a simple neuron having only non-gated, ion selective membrane channels. Of course, this simple neuron is insufficient for describing the complex membrane potential changes of a normal neuron. Hodgkin and Huxley Hodgkin and Huxley (1952d); Hodgkin and Huxley (1952b); Hodgkin

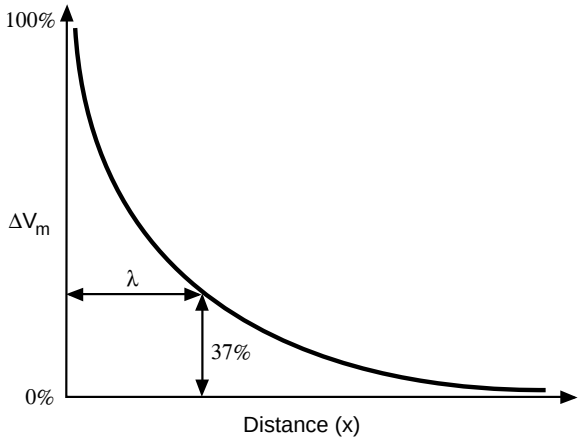

Figure 3: Membrane potential decay with respect to spatial location.

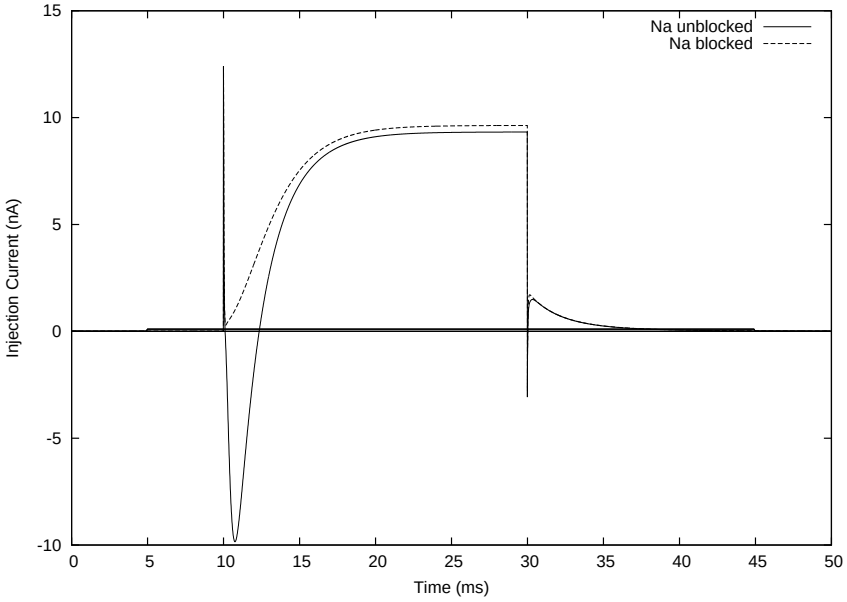

Figure 4: Current injection applied to maintain 50 mV command voltage for 20 ms for both normal squid axon (*Na unblocked*) and squid axon with blocked Na channel.

and Huxley (1952a); Hodgkin and Huxley (1952c) first explained the role of voltage-gated ion channels in neural membrane potential changes. The now legendary experiment, performed on the axon of the giant squid, mathematically elucidated the behavior of Na^+ and K^+ selective voltage-gated channels.

Hodgkin and Huxley noted the complex, non-linear path of membrane current when a command voltage was applied to the giant squid axon. A plot of this classical behavior is depicted in Figure 4 (*Na unblocked*). Given a command voltage step, the current necessary to maintain membrane potential spikes quickly followed by a brief period of stability. This stable period then decays non-linearly before again recovering non-linearly. Hodgkin and Huxley knew *a priori* that Na^+ and K^+ ions were the dominant ionic species involved in the electro-chemical potential of the neural membrane, and they believed that the complex signature observed was actually the superposition of the Na^+ and K^+ ionic current signatures. To validate this hypothesis, they prepared the axon in an extracellular solution absent Na^+ ions. They then tested this preparation under a command voltage step identical to that of the normal neuron. Their resulting injection current trace, shown

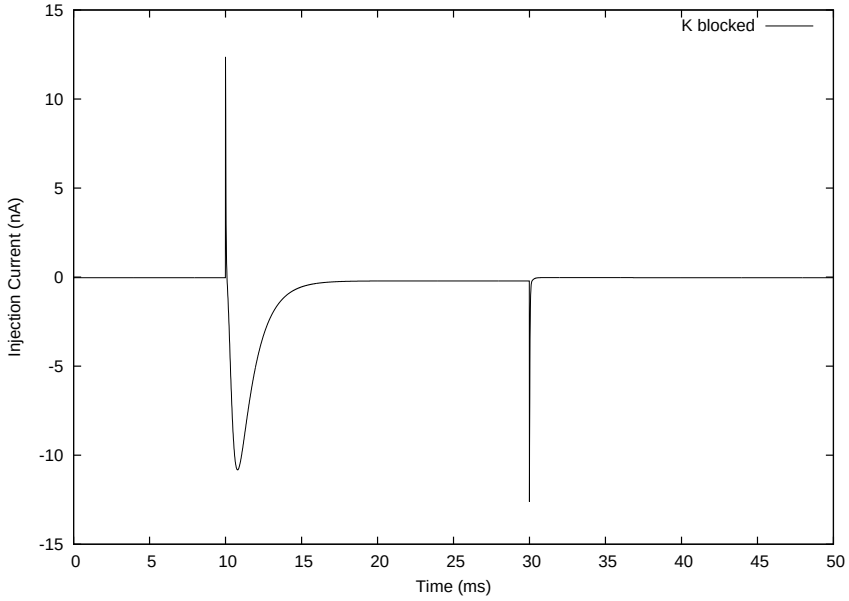

Figure 5: Current injection applied to maintain 50 mV command voltage for 20 ms for squid axon with blocked K channel.

in Figure 4 (*Na blocked*), was that of the behavior of the K^+ ions alone. Subtraction of this plot from the normal neuron plot provided the Na^+ ion current trace which is shown in Figure 5.

Decomposition of Na^+ and K^+ ionic contributions to the membrane current trace was only the initial experimental step. Hodgkin and Huxley performed similar experiments over a wide range of command voltages. Studying the differences in the current signatures, they were able to develop the functional relationship between voltage-gated ionic channel permeability and voltage. A mathematical model based on these findings, widely called the Hodgkin-Huxley model, is described below.

As we have already discussed, an ion channel is an opening in the neural membrane that permits diffusion of ionic species across the membrane barrier. Channels permit ionic passage in either direction. Channels are also selective to particular ionic species, meaning that a channel permitting Na^+ diffusion across the membrane will not permit K^+ diffusion. Non-gated ion channels freely allow passage of ionic species. More formally, non-gated ion channels have constant conductance. Ionic currents passing through these channels directly obey Ohms Law.

Voltage-gated ion channels behave much differently. The conductivity of these channels is a function of membrane potential. As the name would imply, the conductivity of these channel types is gated. Another way to think of this is that the channel itself is door that swings open freely. The gates act as a system of locks keeping the door closed to ionic passage.

Each gate has a probability, a value on the range $[0, 1]$, of being unlocked, which is referred to as the *permissive state*. A particular channel's conductivity may depend on many identical gates and any number of gate types. Formally, conductance is related to these permissive states by the following equation:

$$G_{chan} = \bar{g}_{chan} \prod_i p$$

where p is the probability of a gate being in its permissive state, G_{chan} is the absolute channel conductance per unit membrane area, and $\bar{g}_{chan}$ is the maximal channel conductance possible if all gates were in the permissive state. The product of the probabilities of a permissive state for all gates governing the channel comprises the fraction of maximal conductance possible, thus defining the absolute conductance. We will see that the probability of the permissive state for a gate is a function of voltage. However, first we should introduce practical notation. The vast majority of voltage-gated ion channels are gated by at most three

unique gate types. Thus, the previous equation may be rewritten as:

$$G_{chan} = \bar{g}_{chan} p_1^{x_1} p_2^{x_2} p_3^{x_3}$$

where G_{chan} and $\bar{g}_{chan}$ are defined as previous, $p_i, i = 1, 2, 3$ are the unique gate types, and $x_j, j = 1, 2, 3$, represent the number of gates of each gate type involved in channel gating, respectively.

The rate of change of gate permissiveness with respect to time obeys first order kinetics. This is described mathematically as:

$$\frac{dp_i}{dt} = \alpha_{p_i}(1 - p_i) - \beta_{p_i} p_i$$

where α denotes the activation, or opening, of the gate, and β denotes the inactivation, or closing, of the gate. Both variables, α and β, are functions of membrane potential. Before moving on, it is important to understand this equation exactly. Given some probability of permissiveness, the rate of change of permissiveness with respect to time is increased by the activation rate times the probability of the gate being closed minus the inactivation rate times the probability of the gate being open. The probability of gate permissiveness is always on the range $[0, 1]$. Any product of a value on this range to any power will always be on the range $[0, 1]$. Therefore, even though gate permissiveness may change with respect to time, the channel conductance, as defined above will always vary over the range $[0, \bar{g}_{chan}]$.

Finally, we must specify functional descriptions of the variables α and β with respect to membrane potential. Through careful experimentation, these functions have been approximated for a wide range of voltage-gated channel types. The most commonly encountered channels have gate variables well-approximated by a common function form Bower and Beeman (1997):

$$\frac{A + Bx}{C + exp\left(\frac{x+D}{F}\right)}$$

Given that we have rates of change equations defined for the permissiveness of our gates to ionic diffusion, a question should enter your mind. These gates must have absolute values when solving for channel conductance. Yet we only have equations for rates of change. How do we solve for the values themselves? While the proper answer to this question must wait for a discussion of numerical integration methods, we can solve for gate permissiveness under equilibrium conditions. Given any membrane potential over the range defined for α and β, the steady state value of the gate permissiveness can be determined. This is achieved by setting the derivative of the gate permissiveness equal to zero and solving for the activation and inactivation values at some membrane potential, usually termed, V_{init}. Simple algebraic manipulation of the equation of rate of change yields the following equation:

$$p_{ss} = \frac{\alpha_p}{\alpha_p + \beta_p}$$

where p_{ss} is the steady state permissiveness of gate, p at some voltage, V, and α_p and βp are the activation and inactivation values of gate p at V.

Thus, given any initial membrane potential value, V_{init}, we assume the neuron is not disturbed and achieves equilibrium. Each gate variable permissiveness at this potential may be determined and used as an initial state value of the neuron. With the inclusion of voltage-gated ion channels, we have achieved a formal specification of a biologically-motivated neural membrane.

For illustration, Figure 6 depicts mathematically modeled behavior of Na^+ and K^+ channel activation and inactivation gates for hippocampal CA3 pyramidal cells originally modeled by Traub Traub et al. (1991). In this diagram, the m and h gates govern the Na^+ channel conductance and the n gate controls the K^+ channel conductance. The left-hand plot depicts the rate of change of the gate activation and inactivation variables with respect to membrane potential. Rates of change are measure in ms. The most important point of this figure is to understand that gate variable rates of change are highly non-linear and vary widely. The interplay of these functions produce the complex behavior of the neuron. The right-hand plot depicts the steady state permissiveness of the gates for a range of membrane potentials. As was explained above, these values must vary over the range $[0, 1]$. The steady state plot of gate permissiveness is very powerful in

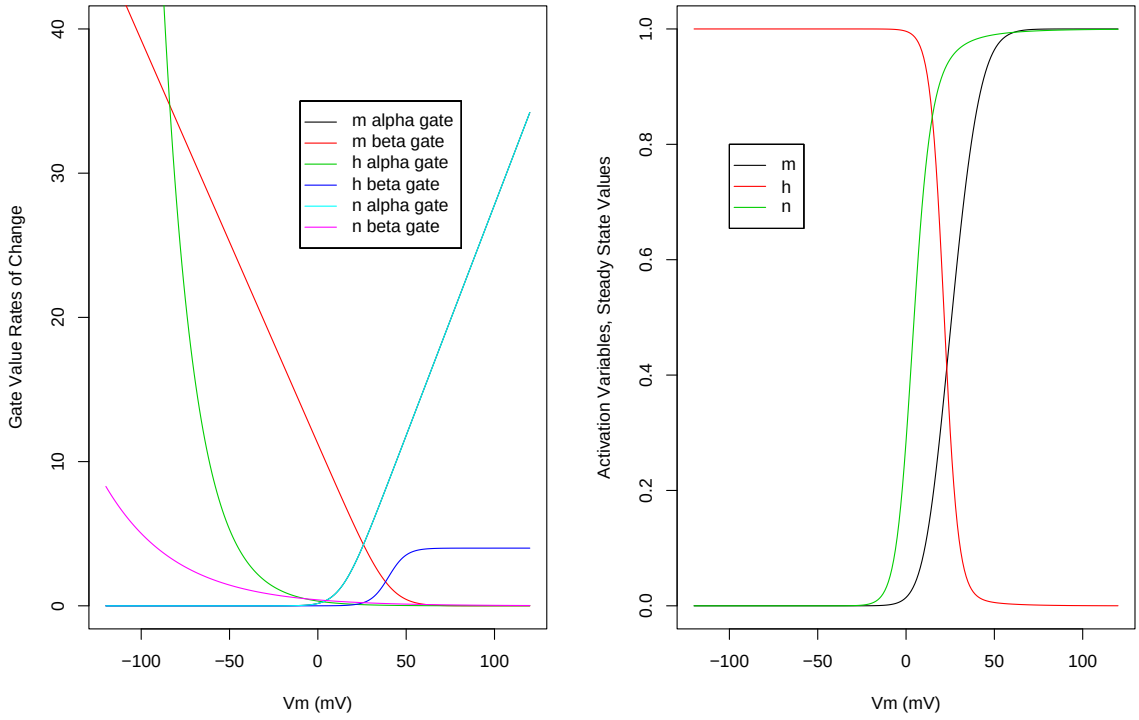

Figure 6: Voltage dependent behavior of (*left*) gate activation and inactivation variable rates of change and (*right*) steady state permissiveness.

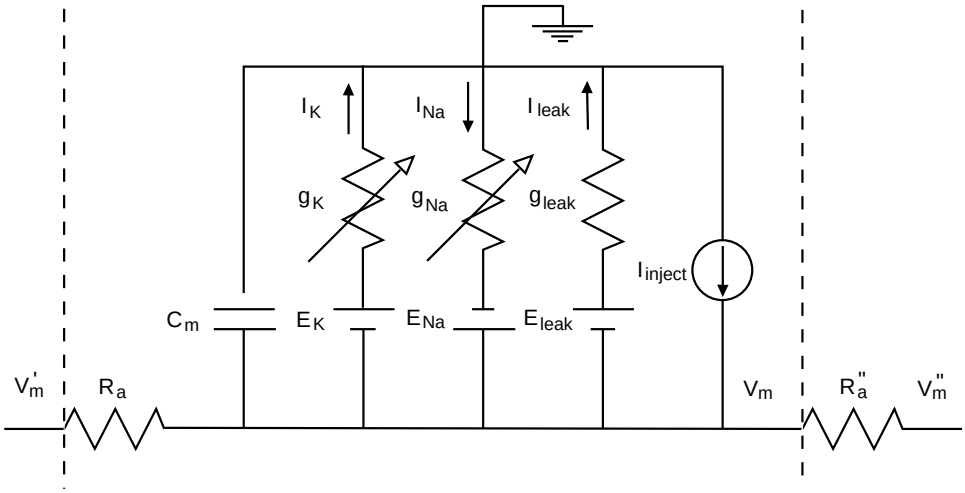

Figure 7: Schematic of a generalized compartment model.

determining the range of membrane potential over which the voltage-gated ion channels governed by these gates will play a role in neural decision functionality.

The importance of the understanding of voltage-gated ion channels in neural modeling cannot be understated. The complex interactions of the gate activation and inactivation equations are the most important influence in membrane potential change of an active neuron during simulation. Inherent understanding of the mathematical premises on which changes take place is crucial to successful modeling.

3.4 The Compartment Model

Now that we have developed the appropriate neurological theory to understand the mechanisms by which neurons maintain membrane potential, as well as how neural membranes respond to the introduction of external currents and potentials both temporally and spatially, we are ready to introduce a formal mathematical neural model on which realistic neural behavior may be simulated.

Canonically, the neural equivalent circuit, or *compartment model*, is used to formally diagram a section of neural membrane. The compartment model circuit incorporating all of the biological features discussed in previous sections is diagrammed in Figure 7.

This circuit diagram represents a single neural compartment. The variables g_K, g_{Na} represent variable conductances of voltage-gated ion channels. The constant conductance g_{leak} is defined as above. R_a represents axial resistance. C_m is membrane capacitance. E_K and E_{Na} represent the reversal potentials (equilibrium potentials) of K^+ and Na^+ non-gated ion channels, respectively. I_{inject} represents externally applicable current sources such as would be used in current and voltage clamp experiments. V_m' and V_m'' variables are provided to illustrate the possible presence of many such compartments. This point raises a major issue in neural modeling. Abstraction of a biological neuron to a computational model requires compartmentalization of the neuron. The number of compartments used determines the accuracy of the model. The mapping of a realistic neural membrane to a compartment model abstraction is illustrated in Figure 8

While a neuron may be roughly approximated by one compartment, it is often advantageous to utilize many compartments connected in serial. The increase in accuracy of a multi-compartment model, however, is often complicated by the absence of realistic neural data to estimate model parameters. This is no small problem. In fact, collection of realistic data for use in parameter approximation is the single most difficult problem in neural modeling. Many of the parameters required to fully specify a computational model are unavailable. Often, parameters from similar or dissimilar neural types are the only data available. Estimation of parameters that are unknown has been labeled the "black art" of computational neuroscience. Knowing when to substitute data taken from dissimilar sources, as well as developing an intuitive feel for good approximate parameter values should be considered an important skill learned with experience. However,

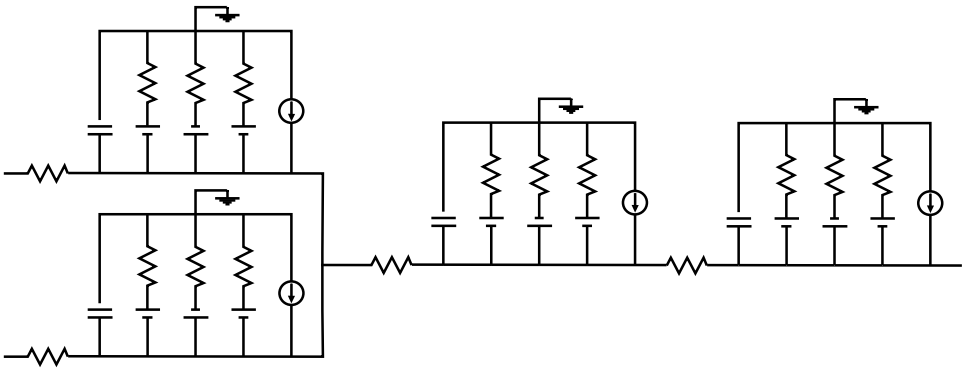

Figure 8: Graphical representation of a complex neural membrane equivalent circuit.

the incorporation of numerical analysis and machine learning techniques for optimizing model parameters given criteria of appropriate behavior should minimize the longevity of this art. Computational tools should, given a set of criteria and bounds on reasonable parameter values, be able to solve for a finite set of optimal model parameters.

Another important principle that should be highlighted here is the importance of units. Once a theoretical model is applied, units become a critical issue. The values supplied as parameters must be mutually consistent with all other values. The two most common sets of units used for neural modeling are base SI (system international) units and biological units, where biological units are a canonical subset of SI units such that model parameters have values close to single or double digits. The use of base SI units often forces parameter specification to be very large or very small such as 15×10^{-6} m and so on. When incorporating units taken from many different sources, make sure the units are consistent, whatever system used.

In addition, the nature of the compartment model should be discussed. We have only described the compartment model as an approximation of neural membrane, but not really what this means. A neuron was previously related to a wire cable. For the purpose of this discussion, we consider a single compartment to model some "segment" of a real neuron. This length takes the form of a cylindrical geometry in most cases (a sphere is often used to approximate the soma). Given this, it should be known that the parameter values specified for the compartment model to this point have not incorporated spatial extent. Conductances are defined in *Siemens*. Resistances have been defined in *Ohms*. When specifying parameters for a computational compartment model, representing a real neuron, these parameters must be specified in terms relative to length, area, and volume. For example, axial resistance is the quantity $Ohms/meter$. Channel conductances are given in $Siemens/meter^2$, and so on. To scale these parameters appropriately, the neural modeler must decide how large a neural section the compartment represents and then assign appropriate units to this geometry.

3.5 Synaptic Connectivity

The complex physiology of the synapse was discussed in Section 2. Fortunately, abstraction of synaptic behavior is rather well-defined when incorporated into models at the compartment level. Almost all synaptic channels have variable conductance that are functions of time. An exception is the case of the NMDA channel which is voltage dependent through the use of an Mg^{2+} ion intermediary. In general, though, the synapse may be modeled by the following equation:

$$I_{syn} = g_{syn}(t)(V_m - E_{syn})$$

I_{syn} is the synaptic current contribution to ionic current, g_{syn} is the time-dependent synaptic conductance and E_{syn} is the reversal potential of the synaptic channel. Other variables are defined as previous. Note, the reversal of the V_m and E_{syn} terms as compared to voltage-gated ion channels. This term reversal has

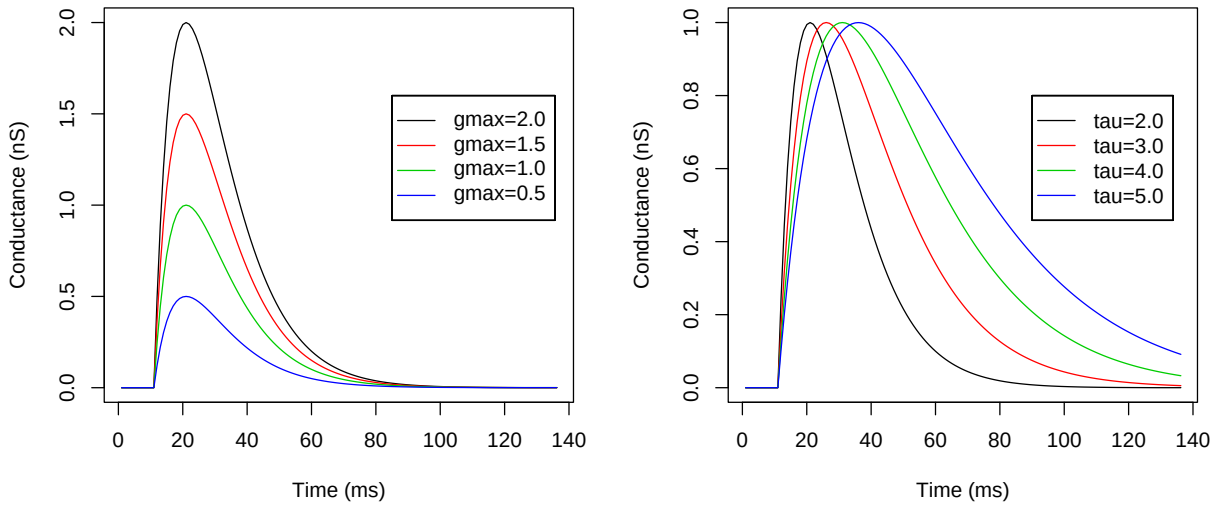

Figure 9: Synaptic channel conductance behavior for the *alpha* function approximation when (*left*) g_{max} is varied ($\tau = 2.0$) and when (*right*) τ is varied ($g_{max} = 1.0$).

important ramifications for the intrinsic value of E_{syn} for each synaptic channel modeled as will be described below.

While seemingly complex, the majority of synaptic channels may be simply described by two function of time, the alpha function and the dual-exponential function. The alpha function is defined by following equation:

$$g_{syn} = g_{max} \frac{t}{\tau} (e^{1-t/\tau})$$

τ is the *time constant* and g_{max} represents the maximum possible conductance of the synapse. Given this description, the notion of *fast* and *slow* behavior is evident. A large value of τ will yield a slow acting synaptic connection. In addition, the g_{max} term will be large for a powerful connection and small for a weak connection. These relationships are depicted in Figure 9.

The *inhibitory* or *excitatory* nature of a synapse is not primarily determined by either the g_{max} or τ term. Rather, the value and sign of the E_{syn} term has greatest influence on the synaptic connections hyperpolarizing or depolarizing influence.

When necessary to describe more complex behavior, the dual-exponential function is used, having the following form Bower and Beeman (1997):

$$g_{syn}(t) = \frac{A g_{max}}{\tau_1 - \tau_2} \left(e^{-t/\tau_1} - e^{-t/\tau_2} \right), \tau_1 > \tau_2$$

where A is a normalizing constant and τ_1 and τ_2 represent the rising and falling *time constants*, respectively. An *AMPA* synaptic connection is well-modeled by the dual-exponential function. Typical values for this connection might be as follows: $g_{max} = 4.8 \times 10^{-9} S, E_{syn} = 0.0V, \tau 1 = 1.0ms, and \tau 2 = 1.0ms$.

3.5.1 NMDA: A voltage gated synapse

Unfortunately, not all synaptic connections commonly used in neural models are as simple as the alpha and dual-exponential functions. *NMDA*, a common slow, excitatory synaptic connection is one such exception.

NMDA conductance is time, voltage, and concentration dependent rather than simply time dependent. The concentration dependence of *NMDA* is mediated by magnesium, $[Mg^{2+}]$, that varies among differing neural types. Traub Traub et al. (1991) described *NMDA* behavior for a CA3 hippocampal pyramidal cell using the following formulation.

$$g_{NMDA} = g_{ligand} \times g_{[Mg^{2+}],V_m}$$

$$g_{ligand} = g_{max} \frac{t}{\tau}(e^{1-t/\tau})$$

$$g_{[Mg^{2+}],V_m} = \frac{1}{1 + \frac{[Mg^{2+}]}{3} \times exp(-0.07(V_m - \xi))}$$

This example underlines the robustness and complexity of nature that must be captured in mathematical models.

3.6 Solving the Discrete Compartment Model

Given the basic mathematical theory of the separate influences on neural compartment potential, we are now ready to assemble the complete mathematical compartment representation. We begin by discussing compartment model parameters as they are often cited in research, as specific units. C_M is specific membrane capacitance, having SI units of F/m^2. R_M is specific membrane resistance having SI units of $Ohm * m^2$. R_A is specific axial resistance having units of $Ohm * m$. Specific quantities are often reported in neural modeling so that they can be studied independent of compartment dimensions, quantities that are often varied.

With specific parameters defined, it is now necessary to convert these quantities into their absolute equivalents. Equations 5, 6, and 7 detail these conversions for a cylindrical compartment.

$$C_m = \Pi dl C_M \tag{5}$$

$$R_m = \frac{R_M}{\Pi dl} \tag{6}$$

$$R_a = \frac{4lR_A}{\Pi d^2} \tag{7}$$

From these absolute units we may redefine the description of passive cable properties representing time τ, and space, λ, constants of the cable as follows.

$$\tau = R_m C_m$$

$$\lambda = \sqrt{\frac{R_m l}{R_a / l}}$$

.

As proposed by Mascagni Mascagni and Sherman (1998) the differential equation describing a passive cable compartment is given by:

$$\lambda^2 \frac{\delta^2 V}{\delta x^2} - \tau \frac{\delta V}{\delta t} - V = 0$$

Substitution of the λ and τ factors yields

$$\frac{R_m l^2}{R_a} \frac{\delta^2 V}{\delta^2} - R_m C_m \frac{\delta V}{\delta t} - V = 0$$

Simple algebraic manipulation yields:

$$C_m \frac{\delta V}{\delta t} = \frac{l^2}{R_a} \frac{\delta^2 V}{\delta x^2} - \frac{V}{R_m}$$

The factor $\frac{\delta^2 V}{\delta x^2}$ may then be discretized by the method of lines Mascagni and Sherman (1998), which assumes that all compartments are of similar geometry and maintain equivalent axial resistance between compartments.

$$C_{m_i} \frac{dV_i}{dt} = \frac{l^2}{R_{a_i}} \frac{V_{i-1} - 2V_i + V_{i+1}}{(\Delta x_i)^2} - \frac{V_i}{R_{m_i}}$$

Obviously, $l = \Delta x$, therefore we may reduce the equation further:

$$C_{m_i} \frac{dV_i}{dt} = \frac{V_{i-1} - 2V_i + V_{i+1}}{R_{a_i}} - \frac{V_i}{R_{m_i}}$$

However, for compartment models in which compartment geometry and size differs, a more robust discrete approximation of the cable model may be derived:

$$C_{m_i} \frac{dV_i}{dt} = \frac{V_{i-1} - V_i}{R_{a_{i-1}}} + \frac{V_{i+1} - V_i}{R_{a_i}} - \frac{V_i}{R_{m_i}}$$

The derivation is that which is most commonly used in neural modeling. The $\frac{V_i}{R_{m_i}}$ resistance based term may be replaced by the more conventional term representing passive membrane conductance per unit area, $\bar{g}_{m_i}$, often called the leak conductance, $\bar{g}_{leak_i}$. It should be noted that if you incorporate membrane resistance based current into your calculations you cannot, realistically, introduce membrane conductance based current influences. These terms are the same and therefore represent a preference in notation. It should also be noted that the $\frac{V_i}{R_{m_i}}$ term is derived for a theoretically based compartment having a rest potential of OmV. As was discussed previously, imbalance of ions maintained by metabolic processes generates a non-zero *rest* potential for a neuron, which is labeled, E_{rest}. Thus, in a neural model in which E_{rest} is non-zero, this passive conductance term is canonically described as $\frac{(E_{leak} - V_i)}{R_{m_i}}$ yielding the generalized passive compartment model:

$$C_{m_i} \frac{dV_i}{dt} = \frac{V_{i-1} - V_i}{R_{a_{i-1}}} + \frac{V_{i+1} - V_i}{R_{a_i}} - \frac{(E_{rest} - V_i)}{R_{m_i}}$$

Adding terms for voltage-gated ion channels and externally applied current yields the overall, generalized compartment equation for potential change with respect to time, Equation 8.

$$C_{m_i} \frac{dV_i}{dt} = \frac{V_{i-1} - V_i}{R_{a_{i-1}}} + \frac{V_{i+1} - V_i}{R_{a_i}} - \frac{(E_{rest} - V_i)}{R_m} + \sum_{chan} \bar{g}_{chan_i}(E_{chan} - V_i) + \sum_{syn} \bar{g}_{syn_i}(E_{syn} - V_i). \quad (8)$$

3.6.1 Numerical Integration

With a spatially discrete mathematical description in hand, the remaining question of modeling becomes one of change with respect to time. As was stated previously, the information of a neuron is not merely membrane potential, but rather how this potential changes with time. Thus, a neural model must accurately simulate membrane potential change given the above equation. To perform this simulation, we must integrate the term $\frac{dV_i}{dt}$ for each compartment with respect to time. The numerical integration process used in a neural model comprises the bulk of the computational process. Primarily, there are three numerical integration techniques used to solve the equation described above: Forward Euler, Backward Euler, and Crank-Nicolson. The first

two techniques are simply opposite approximation techniques. When the term $\frac{dV_i}{dt}$ is discretized to $\frac{V_i^{n+1}-V_i^n}{\Delta t}$, the Forward Euler method requires that all voltage terms on the righthand side be described at time n, which is known

$$C_{m_i}\frac{V_i^{n+1}-V_i^n}{\Delta t} = \frac{V_{i-1}^n-V_i^n}{R_{a_{i-1}}}+\frac{V_{i+1}^n-V_i^n}{R_{a_i}}-\frac{(E_{rest}-V_i^n)}{R_m}+ \sum_{chan}\bar{g}_{chan_i}(E_{chan}-V_i^n)+\sum_{syn}\bar{g}_{syn_i}(E_{syn}-V_i^n)+I_{inject}$$

This type of numerical integration is termed an explicit method, meaning only one unknown variable need be solved, that of V_i^{n+1}. The Backward Euler method is simply the opposite case. All voltage terms on the righthand side are defined for the future time step.

$$C_{m_i}\frac{V_i^{n+1}-V_i^n}{\Delta t} = \frac{V_{i-1}^{n+1}-V_i^{n+1}}{R_{a_{i-1}}}+\frac{V_{i+1}^{n+1}-V_i^{n+1}}{R_{a_i}}-\frac{(E_{rest}-V_i^{n+1})}{R_m}+ \sum_{chan}\bar{g}_{chan_i}(E_{chan}-V_i^{n+1})+\sum_{syn}\bar{g}_{syn_i}(E_{syn}-V_i^{n+1})+I_{inject}$$

The Backward Euler method is an implicit method, as there exists more than one unknown variable to solve given one equation. Solution of an implicit method requires solving all equations for $\frac{V_i^{n+1}-V_i^n}{dt}$ simultaneously. It should be clear that for N compartments, there will exist N equations having 3 unknowns per compartment. This system of linear equations (SLE) forms a tridiagonal matrix which will be discussed in the next section. A second implicit method is the Crank-Nicolson Method which is merely the average of the Forward and Backward Euler methods. The discrete potential derivative form is as follows:

$$\begin{aligned}C_{m_i}\frac{V_i^{n+1}-V_i^n}{\Delta t} = {} & \frac{V_{i-1}^n-V_i^n}{R_{a_{i-1}}}+\frac{V_{i+1}^n-V_i^n}{R_{a_i}}-\frac{(E_{rest}-V_i^n)}{R_m}+ \\ & \sum_{chan}\bar{g}_{chan_i}(E_{chan}-V_i^n)+\sum_{syn}\bar{g}_{syn_i}(E_{syn}-V_i^n)+I_{inject})/2+ \\ & (\frac{V_{i-1}^{n+1}-V_i^{n+1}}{R_{a_{i-1}}}+\frac{V_{i+1}^{n+1}-V_i^{n+1}}{R_{a_i}}-\frac{(E_{rest}-V_i^{n+1})}{R_m}+ \\ & \sum_{chan}\bar{g}_{chan_i}(E_{chan}-V_i^{n+1})+\sum_{syn}\bar{g}_{syn_i}(E_{syn}-V_i^{n+1})+I_{inject})/2\end{aligned}$$

The Forward Euler method, while fastest, is inherently unstable for all but the most prohibitively small time steps, Δt. The Backward Euler method is slow, but inherently stable for all size timesteps Δt. The Crank-Nicolson method is stable, but generally not as slow as the Backward Euler method due to its mathematical properties. The details of this stability are beyond the scope of this paper and readers are referred to Mascagni Mascagni and Sherman (1998) for further information.

Defining these numerical integration formats, however, is not the final step. Rearrangement of terms is still necessary to place the equations in a suitable form for computational solution. A derivation of the tri-diagonal SLE follows for the Backward Euler method. Derivation of the Crank-Nicolson is similar and left as an exercise.

Given the initial Backward Euler form:

$$C_{m_i}\frac{V_i^{n+1}-V_i^n}{\Delta t} = \frac{V_{i-1}^{n+1}-V_i^{n+1}}{R_{a_{i-1}}}+\frac{V_{i+1}^{n+1}-V_i^{n+1}}{R_{a_i}}-\frac{(E_{rest}-V_i^{n+1})}{R_m}+ \sum_{chan}\bar{g}_{chan_i}(E_{chan}-V_i^{n+1})+\sum_{syn}\bar{g}_{syn_i}(E_{syn}-V_i^{n+1})$$

$$\frac{C_{m_i}}{\Delta t}V_i^{n+1} - \frac{V_{i-1}^{n+1} - V_i^{n+1}}{R_{a_{i-1}}} - \frac{V_{i+1}^{n+1} - V_i^{n+1}}{R_{a_i}} + \frac{(E_{rest} - V_i^{n+1})}{R_m} -$$

$$\sum_{chan} \bar{g}_{chan_i}(E_{chan} - V_i^{n+1}) - \sum_{syn} \bar{g}_{syn_i}(E_{syn} - V_i^{n+1}) = \frac{C_{m_i}}{\Delta t}V_i^n + I_{inject}$$

$$\frac{C_{m_i}}{\Delta t}V_i^{n+1} - \frac{V_{i-1}^{n+1}}{R_{a_{i-1}}} + \frac{V_i^{n+1}}{R_{a_{i-1}}} - \frac{V_{i+1}^{n+1}}{R_{a_i}} + \frac{V_i^{n+1}}{R_{a_i}} + \frac{E_{rest}}{R_{m_i}} - \frac{V_i^{n+1}}{R_{m_i}} - \sum_{chan} \bar{g}_{chan_i}E_{chan} +$$

$$\sum_{chan} \bar{g}_{chan_i}V_i^{n+1} - \sum_{syn} \bar{g}_{syn_i}E_{syn} + \sum_{syn} \bar{g}_{syn_i}V_i^{n+1}) = \frac{C_{m_i}}{\Delta t}V_i^n + I_{inject}$$

$$-\frac{V_{i-1}^{n+1}}{R_{a_{i-1}}} + \left(\frac{C_{m_i}}{\Delta t} + \frac{1}{R_{a_{i-1}}} + \frac{1}{R_{a_i}} - \frac{1}{R_{m_i}} + \sum_{chan} \bar{g}_{chan_i} + \sum_{syn} \bar{g}_{syn_i}\right) V_i^{n+1} -$$

$$\frac{V_{i+1}^{n+1}}{R_{a_i}} = \frac{C_{m_i}}{\Delta t}V_i^n + \sum_{chan} \bar{g}_{chan_i}E_{chan} + \sum_{syn} \bar{g}_{syn_i}E_{syn} - \frac{E_{rest}}{R_{m_i}} + I_{inject}$$

$$\varepsilon_i = \frac{\Delta t}{C_{m_i}}$$

$$-\varepsilon_i\frac{V_{i-1}^{n+1}}{R_{a_{i-1}}} + \left(1 + \frac{\varepsilon_i}{R_{a_{i-1}}} + \frac{\varepsilon_i}{R_{a_i}} - \frac{\varepsilon_i}{R_{m_i}} + \varepsilon_i \sum_{chan} \bar{g}_{chan_i} + \varepsilon_i \sum_{syn} \bar{g}_{syn_i}\right) V_i^{n+1} -$$

$$\varepsilon_i\frac{V_{i+1}^{n+1}}{R_{a_i}} = V_i^n + \varepsilon_i \left(\sum_{chan} \bar{g}_{chan_i}E_{chan} + \sum_{syn} \bar{g}_{syn_i}E_{syn} - \frac{E_{rest}}{R_{m_i}} + I_{inject}\right)$$

$$\gamma_i = \varepsilon \left(\sum_{chan} \bar{g}_{chan_i}E_{chan} + \sum_{syn} \bar{g}_{syn_i}E_{syn} - \frac{E_{rest}}{R_{m_i}} + I_{inject}\right)$$

$$-\varepsilon_i\frac{V_{i-1}^{n+1}}{R_{a_{i-1}}} + \left(1 + \frac{\varepsilon_i}{R_{a_{i-1}}} + \frac{\varepsilon_i}{R_{a_i}} - \frac{\varepsilon_i}{R_{m_i}} + \varepsilon_i \sum_{chan} \bar{g}_{chan_i} + \varepsilon_i \sum_{syn} \bar{g}_{syn_i}\right) V_i^{n+1} - \varepsilon_i\frac{V_{i+1}^{n+1}}{R_{a_i}} = V_i^n + \gamma$$

$$\Theta_{L,i} = -\frac{\varepsilon_i}{R_{a_{i-1}}} \tag{9}$$

$$\Theta_{C,i} = 1 + \frac{\varepsilon_i}{R_{a_{i-1}}} + \frac{\varepsilon_i}{R_{a_i}} - \frac{\varepsilon_i}{R_{m_i}} + \varepsilon_i \sum_{chan} \bar{g}_{chan_i} + \varepsilon_i \sum_{syn} \bar{g}_{syn_i} \tag{10}$$

$$\Theta_{R,i} = -\frac{\varepsilon_i}{R_{a_i}} \tag{11}$$

$$\Theta_L V_{i-1}^{n+1} + \Theta_C V_i^{n+1} + \Theta_R V_{i+1}^{n+1} = V_i^n + \gamma_i \tag{12}$$

Equations 9 through 12, for compartments $i = 1, ..., N$ form a system of linear equations which must be solved simultaneously. However, to correctly solve these systems, an additional problem arises. The $\bar{g}_{chan}$

terms are functions of membrane potential, not simply constants. If we utilize the permissiveness rate of change equation with α and β emphasized as functions of potential:

$$\frac{dp_i}{dt} = \alpha(V)_{p_i}(1 - p_i) - \beta(V)_{p_i}p_i$$

Then we may formulate the Backward Euler integration method for this equation as: equation with α and β emphasized as functions of potential:

$$\begin{aligned} \frac{dp_i}{dt} &= \alpha_{p_i}(V_i)(1 - p_i) - \beta_{p_i}(V_i)p_i \\ \frac{p_i^{n+1} - p_i^n}{\Delta t} &= \alpha(V_i^{n+1})_{p_i}(1 - p_i^{n+1}) - \beta_{p_i}(V_i^{n+1})p_i^{n+1} \end{aligned}$$

Algebraic manipulation will yield the following equation:

$$p_i^{n+1} = \frac{p_i^n + \Delta t \alpha_{p_i}(V_i^{n+1})}{1 + \Delta t[\alpha_{p_i}(V_i^{n+1}) + \beta_{p_i}(V_i^{n+1})]} \tag{13}$$

Obviously, Equation 13 has two unknowns, that of potential and permissiveness at a future timestep. Thus, both the future potential and permissiveness must be solved iteratively by the following algorithm:

1. Compute temporary, V_i^{n+1} value using current p_i^n value.
2. Compute temporary, p_i^{n+1} value using temporary V_i^{n+1} value
3. Iterate steps 1 and 2 until the values of V_i^{n+1} and p_i^{n+1} converge (ie. step change is below some relative error value)

3.6.2 Boundary Conditions

The sealed end boundary condition, typically used in solving the types of linear systems described above, requires that no current escape out either end of the cable. This condition can be approximated by assuming the axial resistance at the end compartments approaches infinity. For compartment 1, this causes the $\Theta_{L,1}$ coefficient to be zero. For compartment N, this causes the $\Theta_{R,N}$ coefficient to be zero and the $\Theta_{C,N}$ coefficient to be described as follows:

$$\Theta_{C,N} = 1 + \frac{\varepsilon_i}{R_{a_{i-1}}} - \frac{\varepsilon_i}{R_{m_i}} + \varepsilon_i \sum_{chan} \bar{g}_{chan_i} + \varepsilon_i \sum_{syn} \bar{g}_{syn_i}$$

3.7 Solving Tridiagonal Matrices

For a neuron having N linearly-connected compartments, the implicit Backward Euler method generates a system of linear equations (SLE) to be solved, having a unique form called a tridiagonal matrix. A five compartment neuron SLE is depicted in Equation 14 representing the Backward Euler numerical integration derivation described above.

$$\begin{pmatrix} \Theta_{C,1} & \Theta_{R,1} & 0 & 0 & 0 \\ \Theta_{L,2} & \Theta_{C,2} & \Theta_{R,2} & 0 & 0 \\ 0 & \Theta_{L,3} & \Theta_{C,3} & \Theta_{R,3} & 0 \\ 0 & 0 & \Theta_{L,4} & \Theta_{C,4} & \Theta_{R,4} \\ 0 & 0 & 0 & \Theta_{L,5} & \Theta_{C,5} \end{pmatrix} \begin{pmatrix} V_1^{n+1} \\ V_2^{n+1} \\ V_3^{n+1} \\ V_4^{n+1} \\ V_5^{n+1} \end{pmatrix} = \begin{pmatrix} V_1^n \\ V_2^n \\ V_3^n \\ V_4^n \\ V_5^n \end{pmatrix} + \begin{pmatrix} \gamma_1 \\ \gamma_2 \\ \gamma_3 \\ \gamma_4 \\ \gamma_5 \end{pmatrix} \tag{14}$$

The reason the tridiagonal matrix occurs in compartment modeling arises from the method-of-lines approximation to the second spatial derivative of potential in the cable model. Each compartment potential

depends on its own potential as wells as the left and right neighboring compartments' potentials. The vector of constants arises from the BE derivation incorporating non-voltage dependent terms that are added to the current, known potential. Once in this form, any numerical stable SLE solver may be used. LU Decomposition (Gaussian elimination) is recommended Hines (1989); Mascagni and Sherman (1998).

3.7.1 Concentration Shells

Another common compartment model abstraction is that of the concentration shell, or shell. A shell is a cylindrical volume, having a radial thickness that is measured from the compartment's membrane. This shell acts as a way to abstract the storage and transfer of ions whose concentrations are largely effected by diffusion across the membrane surface. A shell containing ionic species, S, of compartment i is defined as a concentration, $\chi_{S,i}$, an ionic conversion rate, $\phi_{S,i}$, and a concentration decay rate, $\tau_{S,i}$. The units of $\chi_{S,i}$ are $moles/m^3$. The units of $\phi_{S,i}$ are $moles/(m^3 A$ and the units of $\tau_{S,i}$ are sec. The kinetics of concentration are described by Equation 15:

$$\frac{d\chi_{S,i}}{dt} = \phi_{S,i} I_{S,i} - \frac{\chi_{S,i}}{\tau_{S,i}} \tag{15}$$

where $I_{S,i}$ is the ionic current of species, S, in compartment, i. Discretizing this equation using the Backward Euler method gives the following derivation:

$$\begin{aligned}
\frac{\chi_{S,i}^{n+1} - \chi_{S,i}^{n}}{\Delta t} &= \phi_{S,i}^{n+1} I_{S,i} - \frac{\chi_{S,i}^{n+1}}{\tau_{S,i}} \\
\frac{\chi_{S,i}^{n+1}}{\Delta t} + \frac{\chi_{S,i}^{n+1}}{\tau_{S,i}} &= \phi_{S,i}^{n+1} I_{S,i} + \frac{chi_{S,i}^{n}}{\Delta t} \\
\chi_{S,i}^{n+1} \left(\frac{1}{\Delta t} + \frac{1}{\tau_{S,i}} \right) &= \phi_{S,i}^{n+1} I_{S,i} + \frac{\chi_{S,i}^{n}}{\Delta t} \\
\chi_{S,i}^{n+1} \left(1 + \frac{\Delta t}{\tau_{S,i}} \right) &= \Delta t \phi_{S,i}^{n+1} I_{S,i} + \chi_{S,i}^{n} \\
\chi_{S,i}^{n+1} &= \frac{\Delta t \phi_{S,i}^{n+1} I_{S,i} + \chi_{S,i}^{n}}{1 + \frac{\Delta t}{\tau_{S,i}}}
\end{aligned} \tag{16}$$

Given the derived Backward Euler update, Equation 16, solutions of $\chi_{S,i}$ for all species, S, and all compartments, i, must be addressed at each time step. Moreover, if channels are gated on value of $\chi_{S,i}$ then it must be updated during convergence of compartment potential over a timestep.

3.8 Units Conversion Table

Relevant SI Units				
Quantity	Name	Symbol	Units	Base Units
Capacitance	Farads	F	C/V	$m^{-2}kg^{-1}s^2Q^2$
Charge	Coulombs	Q	$A * s$	Q
Conductance	Siemens	S	Ω^{-1}	$m^{-2}kg^{-1}sQ^2$
Current	Amperes	A	Q/s	Q/s
Length	Meters	m	m	m
Potential	Volts	V	V	$m^2kgs^{-2}Q^{-1}$
Resistance	Ohms	Ω	S^{-1}	$m^2kg^1s^{-1}Q^{-2}$
Time	Seconds	s	s	s

References

Bower, J., & Beeman, D. (1997). *The Book of Genesis*. Springer-Verlag, New York, NY.

Hines, M. (1989). A program for simulation of nerve equations with branching geometries. *Int. J. Biomed. Comput.*, 24:55–68.

Hodgkin, A., & Huxley, A. (1952)a. The components of membrane conductance in the giant axon of loligo. *J. Neurophysiology*, 116:473–496.

Hodgkin, A., & Huxley, A. (1952)b. Currents carried by sodium and potassium ions through the membrane of the giant axon of loligo. *J. Neurophysiology*, 116:449–472.

Hodgkin, A., & Huxley, A. (1952)c. The dual effect of membrane potential on sodium conductance in the giant axon of loligo. *J. Neurophysiology*, 116:497–506.

Hodgkin, A., & Huxley, A. (1952)d. A quantitative description of membrane current and its application to conduction and excitation in nerve. *J. Neurophysiology*, 117:500–544.

Kandel, E., Schwartz, J., & Jessell, T. (1991). *Principles of Neural Science*. Appleton and Lange, East Norwalk, CT.

Mascagni, M., & Sherman, A. (1998). Numerical methods for neuronal modeling. In *Methods of Neuronal Modeling: From Ions To Networks*, pages 569–606, Cambridge, MA. MIT Press.

Traub, R., Wong, R., Miles, R., & Michelson, H. (1991). A model of a CA3 hippocampal pyramidal neuron incorporating voltage-clamp data on intrinsic conductances. *J. Neurophysiology*, 66:635–650.